Ancient TL

www.ancienttl.org · ISSN: 2693-0935

Clark-Balzan, L., 2016. *Source and characteristics of blue, infrared (IR), and post-IR IR stimulated signals from gypsum-rich samples.* Ancient TL 34(1): 6-13.
https://doi.org/10.26034/la.atl.2016.499

Ancient TL

Source and characteristics of blue, infrared (IR), and post-IR IR stimulated signals from gypsum-rich samples

Laine Clark-Balzan[1*]

[1] Institute of Earth and Environmental Sciences, Geology, Albert-Ludwigs-Universität
Albertstr. 23-B, Freiburg, 79104, Germany

*Corresponding Author: laine.clark-balzan@geologie.uni-freiburg.de

Received: May 1, 2016; in final form: June 3, 2016

Abstract

Samples collected from gypsiferous deposits in the Nefud Desert, Saudi Arabia, yielded anomalous signals when presumed quartz and feldspar extracts were measured with BSL and $pIRIR_{290}$ SAR protocols, respectively. Subsequent scanning electron microscopy analysis indicated that the majority of extracted coarse grains were gypsum instead of quartz or feldspar. Luminescence signals were detected from gypsum at room or low (50 °C) temperature when stimulated with blue (UV detection: 330, 380 nm) or IR (blue detection) light. No UV (330 nm) emissions were detected with IRSL stimulation. A modified SAR protocol (no preheats) was successful in building saturating exponential growth curves for BSL/UV_{380} and IRSL/blue emissions from gypsum, with acceptable recycling and zero ratios. Luminescence measurement of gypsum with standard protocols used for quartz (BSL/UV_{340} SAR with preheats) and feldspar ($pIRIR_{290}$ with preheats) yielded either negligible or anomalous signals that could be excluded from consideration via typical rejection criteria. Additionally, massive decrease in sensitivity with SAR cycle was found to be indicative of gypsiferous content. Therefore measurement of quartz and feldspar aliquots according to standard procedures should be possible even in gypsum-contaminated samples, though concentration of these minerals via an extra density separation step may be necessary.

Keywords: luminescence, gypsum, sample preparation, rejection criteria

1. Introduction

Gypsum ($CaSO_4 \cdot 2H_2O$) is a moderately soluble evaporite commonly found in arid environments. Precipitate deposits may be classified as primary, forming from a supersaturated brine pool, secondary, precipitating in intrasedimentary spaces (e.g. desert roses), or, perhaps most often, a mixture of the two (Warren, 2006). Unless gypsum has formed within a supersaturated water column, mineral inclusions such as quartz and feldspar grains are very common, and physical separation of the minerals is complex and time-consuming (McLeod et al., 1985). Anhydrite ($CaSO_4$) is a closely related mineral that may form naturally, or it can be produced artificially by heating gypsum and inducing the progressive loss of both water molecules. Loss of water from the crystal structure begins at temperatures as low as ∼363 K (∼90 °C) (Lager et al., 1984).

Various attempts have been made to date gypsum or anhydrite via trapped charge dating techniques, such as electron spin resonance and thermoluminescence (Nambi, 1982; Mathew et al., 2004; Nagar et al., 2010; Aydaş et al., 2011). More recently, O'Connor et al. (2011) have shown that room temperature blue light stimulation (470 ± 30 nm) and infrared stimulation (830 ± 10 nm) of both gypsum and anhydrite yield measurable UV (5 mm Hoya U-340) or blue-violet (1 mm Schott BG-39 and 2.5 mm Corning 7-59) and UV emissions. Detschel & Lepper (2009) also detected BSL/UV and IRSL/UV signals (same stimulation/detection as above) from gypsum at room temperature, but only BSL/UV from anhydrite. The irradiating source in this study, however, was ionizing UV radiation from a deuterium source, therefore it may not be directly comparable. O'Connor et al. (2011) also reported that a modified, room temperature SAR protocol adequately corrected for sensitivity changes and could be used to measure a saturating exponential regeneration curve, how-

ever, signal fading was significant (less than 5 % per decade) for all tested combinations except for IRSL/UV of gypsum. Jain et al. (2006) published measurable signal and growth curves from gypsum and anhydrite (BSL/UV), but noted a sensitivity decrease of nearly an order of magnitude after preheating to 260 °C (held 0 s). Mahan & Kay (2012) attempted to date gypsum from Salt Basin Playa via a BSL/UV SAR protocol with preheats of 180 °C for 10 s and BSL measurement at 125 °C, working on the assumption that the complete transformation into anhydrite did not occur until ca. 180 – 200 °C. They also noted severely decreased signal intensity with preheats greater than this temperature. Standard preheats or raised temperature stimulations seem to have a deleterious effect on the signals measured from gypsum, which is likely linked to dehydration of the crystal structure and eventual conversion to anhydrite. It should be emphasized that the above research has shown anhydrite and gypsum to have distinct signal characteristics (Detschel & Lepper, 2009; Jain et al., 2006) and fading rates (O'Connor et al., 2011).

Samples collected from gypsum-rich environments are likely to comprise mineral mixtures which cannot be completely separated, and the experiments described above suggest that gypsum/anhydrite may produce a measurable emission during standard, elevated temperature OSL/IRSL measurement of quartz or feldspar. Luminescence signal contamination can lead to age underestimation if a proportion of the measured signal fades over geological time scales. It may also lead to incorrect dose rate calculations if radioisotope distribution and attenuation factors are miscalculated or poorly understood. Current rejection criteria, such as the IR depletion ratio (Duller, 2003), ensure that feldspar dominated aliquots are excluded from quartz BSL populations, while IRSL emissions from quartz will be negligible during typical feldspar IRSL and elevated temperature post-IR IRSL measurements (Spooner, 1994). The efficacy of such measures for excluding gypsum- or anhydrite-signal dominated aliquots, however, has not been tested.

2. Methodology

Samples were collected from two endorheic basins, Al Marrat and Jubbah, located near the southern edge of the An Nefud sand sea (Saudi Arabia) (Petraglia et al., 2011, 2012). Gypsum-rich samples (JB2-OSL2: 1.57 m, JB2-OSL5: 4.15 m) were collected from palaeoenvironmental sampling site JB-2 in the Jubbah basin, an 8.5 m section comprising carbonate-rich and gypsiferous sediments, sands, and clays. Field observations indicated extensive gypsum precipitation within the upper four to five meters of this section, with crystals up to several centimeters in size. During sampling, however, an effort was made to avoid the most gypsiferous units, and samples were collected from powdery carbonate units. It was presumed that these carbonate units might be more likely to include quartz and feldspar grains. Collection and initial preparation methods for nominal 'quartz' and 'feldspar' coarse grain fractions (180 – 255 µm) followed Hilbert et al. (2014), and included wet sieving, digestion in hydrochloric acid, a sodium polytungstate separation (ρ = 2.58 g cm^{-3}), and ninety minutes hydrofluoric acid etching for the quartz fraction.

Subsequently, these samples were prepared with a second sodium polytungstate separation (ρ = 2.35 g cm^{-3}) in order to further separate pure gypsum crystals. The efficacy of these density separations will be discussed later. In the results and discussion, mineral fractions will be referred to by density (e.g. $\rho < 2.58$ or $\rho < 2.35$ g cm^{-3}). Typical Nefud coarse-grained quartz (Q) and feldspar (F) separates (180 – 255 µm) were extracted from luminescence samples collected in sand-rich deposits in the nearby Al Marrat basin and Jubbah basin site Al-Rabyah (Hilbert et al., 2014), respectively. These were prepared according to the first method described above.

All equivalent dose (D_E) measurements were performed with either a lexsyg research or a lexsyg smart (Richter et al., 2013). Standard BSL SAR (Murray & Wintle, 2000, 2003), $pIRIR_{290}$ SAR (Thiel et al., 2011), and modified low temperature BSL and IRSL SAR protocols (similar to

Set	Stim./Detection	Use	Filters
1	BSL/UV_{340}	Standard BSL SAR	Hoya U340 glass (2.5 mm) + Delta-BP 365/50 EX-interference (5 mm)
2	$IRSL\&pIRIR_{290}$	Standard $IRSL_{50}$ and $pIRIR_{290}$	Schott BG 39 glass (3 mm) + AHF Brightline HC414/46-interference (3.5 mm)
3	BSL/UV_{330}	Gypsum characterization (RT)	Hoya U340 glass (2.5 mm) + AHF Brightline HC340/26 Interference (5 mm)
4	BSL/UV_{380}	Gypsum characterization (RT)	Hoya U340 glass (2.5 mm) + Delta-BP 365/50 EX-Interference (5 mm)
5	$IRSL/UV_{330}$	Gypsum characterization (50 °C)	Hoya U340 glass (2.5 mm) + AHF Brightline HC340/26 Interference (5 mm)
6	IRSL/blue	Gypsum characterization (50 °C)	Schott BG 39 glass (3 mm), Schott BG 25 (3 mm), Schott KG3, (2 mm)

Table 1. Filter combinations used for measurements.

O'Connor et al. 2011) were tested for various mineral fractions. Measurement parameters and luminescence signal integration limits are given in Tables 1 and 2, and data were analysed with Luminescence Analyst v. 4.11. Detection/emission combinations are referred to in the text as, e.g., BSL/UV_{330}: blue light stimulation with emission detection centered at 330 nm. Though the gypsum will be at least partially dehydrated by heating, we will refer to non-quartz and feldspar aliquots both pre- and post-heating as either gypsum or gypsum-rich.

3. Results and Discussion

Initial BSL and $pIRIR_{290}$ measurements upon mineral separates ($\rho < 2.58$ g cm^{-3} and $\rho < 2.58$ g cm^{-3}, respectively) from samples JB2-OSL1 and JB2-OSL2 yielded either negligible or anomalous signals (see discussion below and Figure 3). This prompted the mineralogical investigations and luminescence characterization reported here. As a first step, the purity of each fraction was investigated via scanning electron microscopy. Previously measured aliquots from both samples were carbon coated and examined for grain morphology and composition. Many crystals displayed morphology typical of gypsum (Mees et al., 2012), with elongated shapes (> 600 µm) or smaller, broken crystal forms (Figure 1). Spectral analysis confirmed the dominant presence of gypsum with some quartz or feldspar grains in both fractions. Nominal 'quartz' aliquots ($\rho > 2.58$ g cm^{-3}) comprised half or more gypsum grains, while nominal 'feldspar' aliquots ($\rho < 2.58$ g cm^{-3}) comprise primarily gypsum, with infrequent feldspar and quartz grains. Mahan & Kay (2012) also described poor results from density separation of gypsum-rich samples and attributed this to gypsum overgrowth upon denser minerals such as quartz. It seems possible, too, that the sheer amount of gypsum in these samples might have trapped denser grains during density separation, though samples were stirred gently to discourage grain clumping and then centrifuged for at least 5 minutes. It can also be noted that SEM images of the gypsum crystals do not show any pits indicative of hydrofluoric or hydrochloric acid etching. Gypsum reaction with hydrofluoric acid seems to be negligible at room temperature during the 90 minute etch used here; this is in contrast to HF etching of quartzes and feldspars which results from the conversion of silicates into fluorosilicates (Fogler et al., 1975). Indeed, chemical removal of gypsum precipitates requires extensive treatment with high strength acids, for instance, treatment by ethylene diamine tetra acetic acid followed by digestion in heated 12 N HCl for three hours (Kocurek et al., 2007; Mahan & Kay, 2012).

We then confirmed that these gypsum-rich aliquots ($\rho < 2.58$ g cm^{-3}, sample JB2-OSL5) yielded a luminescence signal if measured at room temperature (RT). Three aliquots (6 mm diameter) were bleached with both blue (100 s) and IR LEDs (300 s) at room temperature, after which each underwent several cycles of irradiation (27.8 Gy) and luminescence detection with various stimulation/emission parameters (Tables 1 and 2): BSL/UV_{330}, BSL/UV_{380}, IRSL/UV_{330}, and IRSL/blue. Luminescence decay curves are shown in Figure 2a. Absolute signal strength and relative magnitude of the tested signals were similar for all three aliquots. BSL/UV_{380} provided the strongest signal, with an initial magnitude of approximately 1000 counts per 0.1 s. BSL/UV_{330} was the next strongest, with a signal approximately 60 % of the BSL/ UV_{380} signal, followed by IRSL/blue (20 %). IRSL/UV_{330} provided by far the weak-

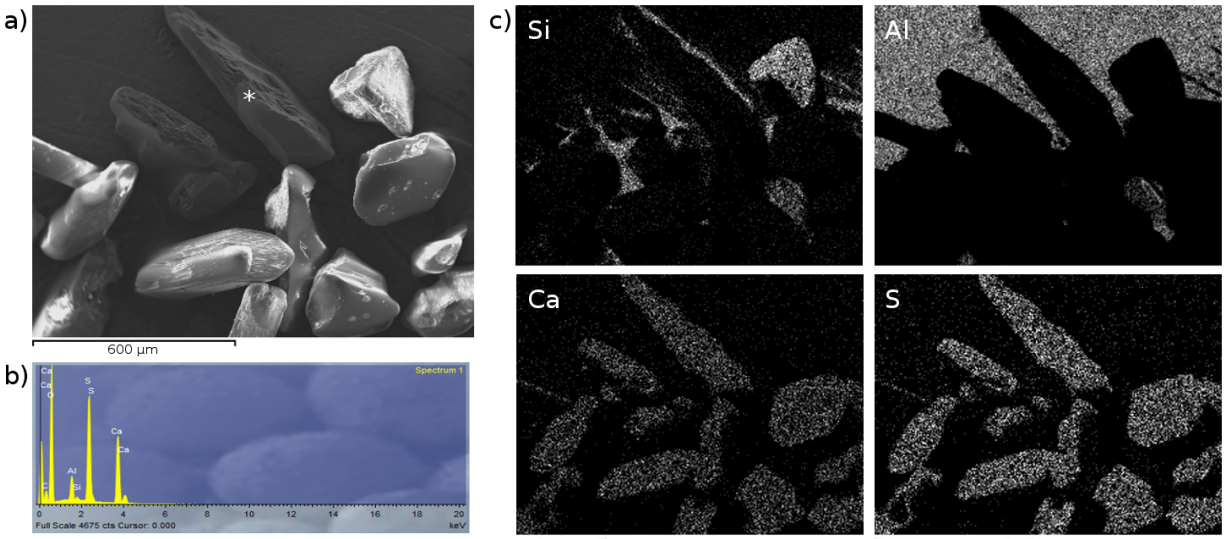

Figure 1. SEM image of JB2-OSL5 aliquot ($\rho < 2.58$ g cm^{-3}). Nearly all of the crystals in the view are gypsum, based on the elemental compositions shown in (c) and crystal morphology. The spectrum shown in b) was collected at the point marked with the white star in a). The crystal on the upper right is quartz, and no feldspars are visible. Silicon rims around many of the grains are due to the use of silicone oil in aliquot preparation.

SAR Step	Standard BSL	$pIRIR_{290}$	Modified BSL	Modified IRSL
1	β irradiation	β irradiation	β irradiation	β irradiation
2	Preheat 260 °C (5 °C s^{-1}, hold 10 s)	Preheat 320 °C (5 °C s^{-1}, hold 60 s)	Pause 10000 s	
3	IRSL (IR depletion step only) 50 °C, 100 s	IRSL[2] 50 °C, 200 s Signal: first 2 s Background: last 50 s	BSL[4] RT, 100 s stimulation Signal: first 1.5 s Background: last 30 s	IRSL[6] 50 °C, 300 s Signal: first 2.5 s Background: last 100 s
4	BSL[1] 125 °C, 60 s Signal: first 0.2 s Background: last 20 s	IRSL[2] 290 °C, 200 s Signal: first 2 s Background: last 50 s		
5	β irradiation	β irradiation	β irradiation	β irradiation
6	Preheat 240 °C (5 °C s^{-1}, hold 10 s)	Preheat 320 °C (5 °C s^{-1}, hold 60 s)	Pause 10000 s	
7	BSL[1] As above	IRSL[2] 50 °C as above	BSL[4] As above	IRSL[6] 50 °C as above
8	Hot Bleach 280 °C, 100 s blue LED stimulation	IRSL[2] 290 °C as above		
9		Hot Bleach 325 °C, 100 s IR LED stimulation		

Table 2. Stimulation and heating parameters for regeneration protocols. Aliquots were prepared in the following sizes (left to right): 2 mm, 1 mm, 6 mm, 6 mm.

est signal, with a relative strength of only 3 %. In all cases, a significant BSL signal could still be measured after IRSL stimulation.

Regeneration curves were then measured for both BSL/UV_{380} (RT) and IRSL/blue combinations (50 °C, Figure 2b), using a modified SAR protocol with no preheat (Table 2). For comparison, representative growth curves are shown for typical quartz (BSL SAR with preheat) and feldspar ($pIRIR_{290}$) aliquots as well. It is evident that both gypsum regeneration curves have a higher D_0 than Nefud quartz or feldspar samples, with the IRSL/blue curve yielding the highest saturation point. The highest dose given in the laboratory was 1113 Gy, at which point the normalized IRSL/blue signal was not yet saturated. The D_0 calculated for this aliquot was ca. 1500 Gy. Recycling ratios for both regeneration curves were within two sigma of unity (IRSL/blue: 1.16 ± 0.10; BSL/UV_{380}: 0.99 ± 0.05). Recuperation levels were also low, being negative for IRSL/blue detection and only 5.7 ± 0.9 % for BSL/UV_{380}.

It seems probable that these signals derive primarily from gypsum rather than quartz or feldspar inclusions. Based on SEM results, we know that rare quartz and feldspar grains are included in this fraction, however, no feldspar or quartz grains were identified when aliquots were inspected under a microscope. Of course, this cannot rule out the presence of microscopic mineral inclusions. Yet recorded luminescence characteristics correspond closely to those reported in the literature for natural and synthetic gypsum (Detschel & Lepper, 2009; O'Connor et al., 2011). Examination of TL measurements for several aliquots from this fraction did not show a measurable 110 °C peak (i.e. an indication of the presence of quartz grains). Finally, another aliquot of the purified gypsum fraction ($\rho < 2.35$ g cm^{-3}, sample JB2-OSL5) was prepared, irradiated (524.4 Gy), and its luminescence signal was measured with an EMCCD camera incorporated into a lexsyg research at the Stockholm Luminescence Laboratory (IRSL stimulation at 50 °C, 1.9 s exposure, blue filter set). No emission centers were detected in the resulting image, suggesting that no feldspar inclusions are present; by comparison another gypsum-rich sample with suspected feldspar inclusions was measured and multiple, bright IRSL responsive grains were detected. All evidence suggests that quartz and feldspar inclusions seem to be rare in JB2-OSL5 gypsum grains. Based on grain morphology, we suspect that the most of this sample's gypsum crystallised within a water column and limited the presence of mineral inclusions, however, more research is necessary to prove this.

We then tested the gypsum's luminescence response to typical elevated temperature BSL with preheating, as is often used for quartz luminescence dating. Two aliquots were prepared from the purified gypsum fraction ($\rho < 2.35$ g cm^{-3}, JB2-OSL5) and measured with a full SAR BSL protocol (Tables 1 and 2, Figure 3a). Additionally, twelve aliquots of the primarily gypsiferous 'heavy' fraction ($\rho > 2.58$ g cm^{-3} JB2-OSL2) were prepared and measured with variable stimulation power and integration time (50 or 100 mW cm^{-2}, 0.1 s or 0.5 s per channel). For this second group, only the natural signal and one regeneration dose (152.4 Gy) were measured, with a test dose of 30.5 Gy. All aliquots shared the same characteristics, therefore they are discussed together.

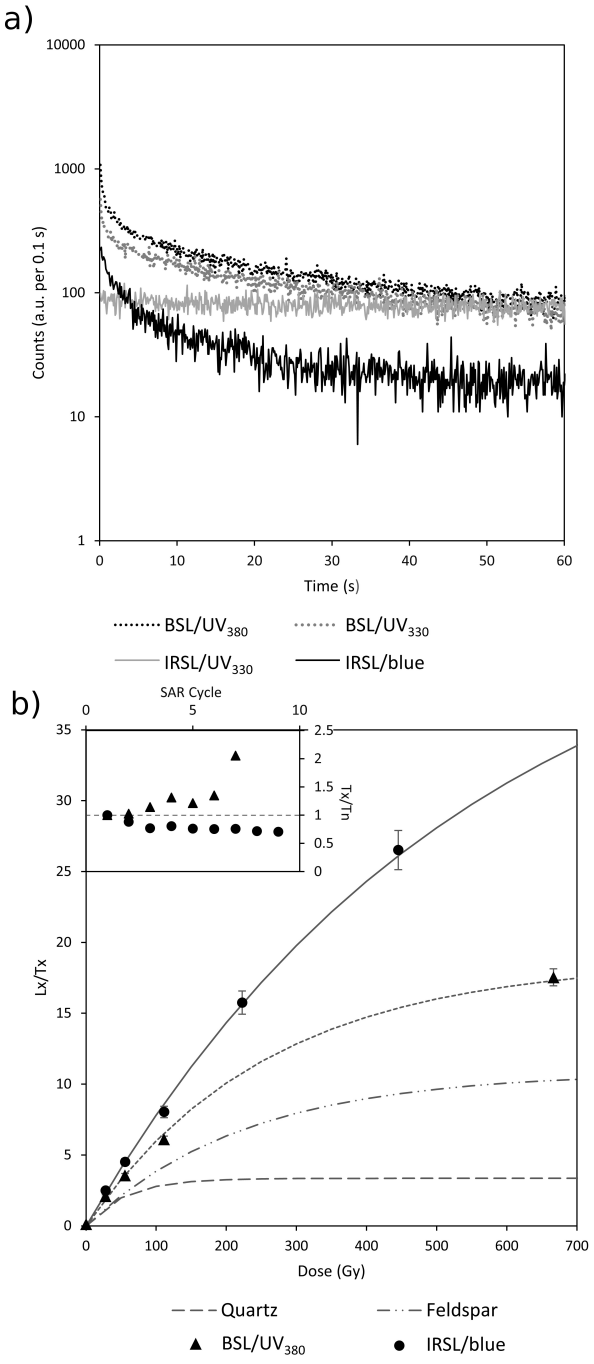

Figure 2. Gypsum luminescence signals. A) Luminescence decay curves recorded at room temperature with various stimulation/detection combinations. B) Regeneration curves and test dose sensitivity changes (inset) measured for gypsum at low temperature (BSL/UV_{380} at room temperature, IRSL/blue at 50 °C) compared to typical quartz BSL/UV_{340} and feldspar $pIRIR_{290}$ curves.

Natural signals of the gypsum-rich separates measured via the typical BSL/UV_{340} quartz SAR protocol were measurable but insignificant. A small initial signal is present (on the order of 150 counts per 0.1 s), but this is more than an order of magnitude less intense than the signal from a typical pure quartz aliquot (Figure 3a). Test doses of up to 29.8 Gy did not yield measurable signals (greater than 3 times the standard deviation above the background level), therefore such aliquots would typically be rejected according to standard rejection criteria. Regeneration doses did produce higher signal levels (e.g. 200 counts per 0.1 s after 299.9 Gy irradiation) however, no growth curve could be constructed due to the lack of test dose signal. By contrast, the reference quartz aliquot yields measurable test dose signals with increasing sensitivity, a regeneration curve well fit by a saturating exponential, good recycling ratio and zero ratios, with no evidence for feldspar contamination (IR depletion ratio). Based on these characteristics, it is unlikely that the low-strength gypsum signal will adversely affect D_E's measured from accepted quartz aliquots. In the case that mineral separation is very poor and only one or a very few quartz grains are included in an aliquot, we suggest that the test dose sensitivity change can be a useful additional rejection criterion. Evidence discussed below and results from Jain et al. (2006) and Mahan & Kay (2012) indicate that a gypsum-dominated signal will show a precipitous decrease in sensitivity after heating to such temperatures, whereas quartz usually increases sensitivity through the SAR cycle (Jungner & Bøtter-Jensen, 1994; Murray & Wintle, 2000).

Two more aliquots were prepared from the purified gypsum fraction ($\rho < 2.35$ g cm^{-3}, JB2-OSL5) and measured according to the $pIRIR_{290}$ protocol (Tables 1 and 2). Ten aliquots each from JB2-OSL2 and JB2-OSL5 ($\rho < 2.58$ g cm^{-3}) were also measured via $pIRIR_{290}$. As above, luminescence characteristics were similar for all three sets of aliquots, therefore they are discussed together.

No signal was detected during IRSL (50 °C) stimulation in either the natural or regenerated measurements; the signal is noisy and never greater than 50 counts per 0.4 s (Figure 3, inset). This value is less than the typical background level of a known feldspar aliquot after 200 s stimulation. When subjected to a subsequent IRSL stimulation at 290 °C, however, gypsum-rich aliquots yield a detectable signal of approximately 500-1000 counts per 0.4 s (Figure 3). The form of this decay is quite different from a typical $pIRIR_{290}$ feldspar signal, and seems to consist entirely of medium and slow components (though no deconvolution was performed). The $pIRIR_{290}$ signal of gypsum also differs from feldspar in that sensitivity dramatically decreases through the SAR cycle: after seven cycles the magnitude of the test dose signal may be ∼10 % or less of the first test dose. High thermal recuperation, between 20 % and 60 % of L_N/T_N ($\mu \pm \sigma$: 41.6 ± 9.8 %), is also a consistent feature.

4. Conclusions

It is important to note that gypsum-rich aliquots yield a detectable signal of approximately 500 – 1000 counts per 0.4 s when measured with IRSL stimulation at 290 °C. We suggest, however, that pure or nearly pure luminescence signals from quartz and feldspar minerals can be detected via the application of standard rejection criteria to BSL/UV_{340} and $pIRIR_{290}$ SAR data, respectively. Aliquots with a sig-

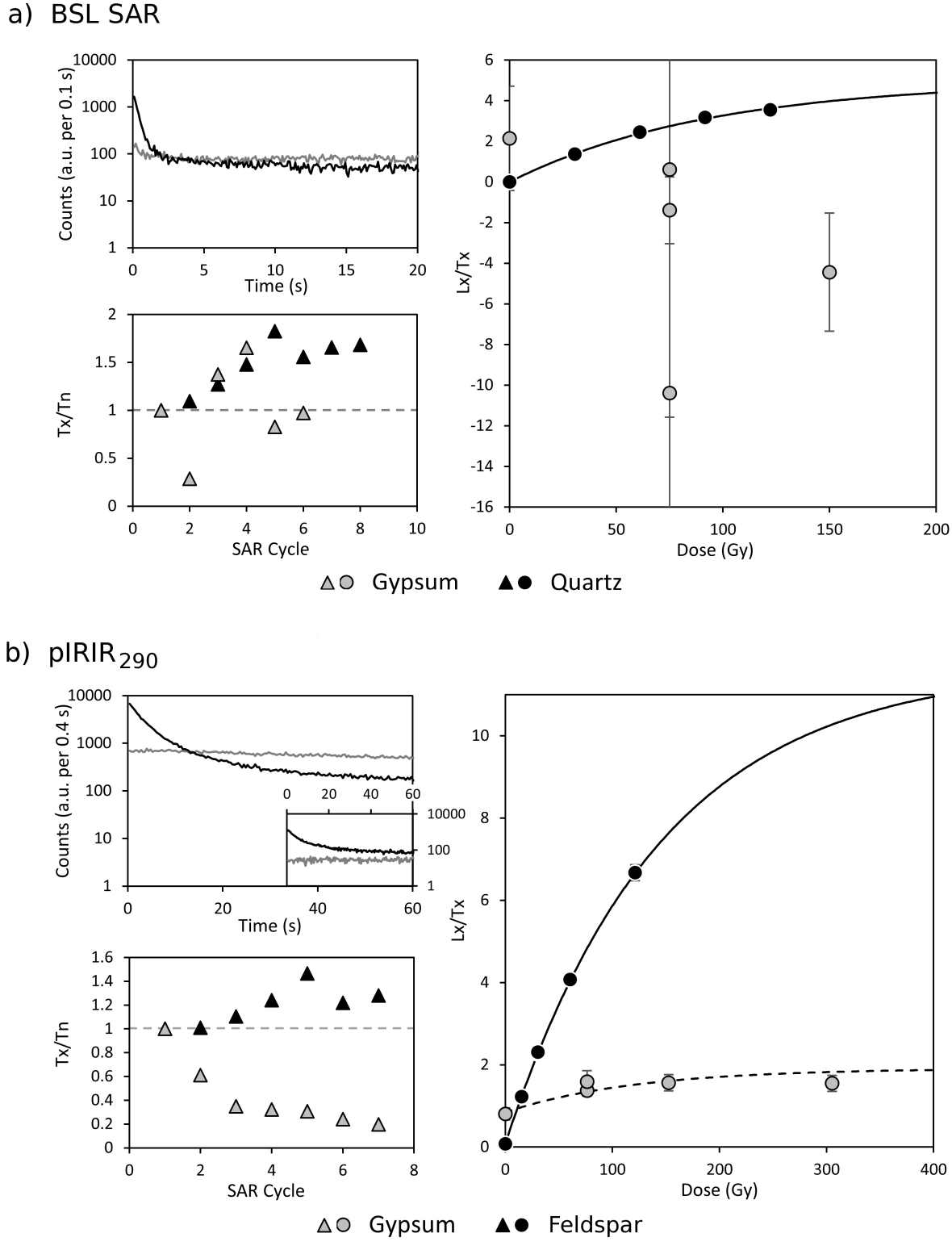

Figure 3. Gypsum-rich aliquots measured with standard BSL/UV_{340} SAR protocol (a) and $pIRIR_{290}$ protocol (b). Gypsum natural decay curves, test dose sensitivity changes, and regeneration curves are plotted in comparison to quartz (a) or feldspar (b). The inset box in (b) shows the natural IRSL (50 °C) signal. Note that several higher regenerated doses (gypsum) are not shown.

nal dominated by gypsum will fail several rejection criteria, particularly:

- detectable natural test signal greater than three sigma above the background signal (BSL)
- test dose error less than 15 – 20 % of the calculated test dose (BSL)
- calculated zero-ratio less than 5 % of L_N/T_N ($pIRIR_{290}$)

Inspection of the decay curve form and test dose sensitivity change should also be conducted if gypsum contamination is suspected, and aliquots with significant sensitivity decrease excluded from further consideration. It may still be prudent to be wary of dates calculated for either quartz or feldspar minerals extracted from a gypsiferous layer if gypsum overgrowth occurs. Grain size estimates are important for attenuation factors and the calculation of internal dose rates for K-feldspars. Gypsum overgrowth will also inhibit hydrofluoric acid etching of quartz, which may lead to dose rate inaccuracies. This issue must be evaluated for each site, however, and is outside the scope of this paper.

Acknowledgments

We thank HRH Prince Sultan bin Salman, President of the General Commission for Tourism and Antiquities, and Professor Ali I. Al-Ghabban, Vice President for Antiquities and Museums, for permission to carry out this study. We also thank Jamal Omar and Sultan Al-Fagir of the Saudi Commission for Tourism and National Heritage (SCTH), and the people of Jubbah for their support and assistance with the field investigations. We acknowledge financial support from the European Research Council (grant no. 295719, to Michael Petraglia) and from the SCTH. Finally, we thank Chris Doherty of the Research Laboratory for Archaeology and the History of Art (University of Oxford) for his assistance with the SEM and Professor Frank Preusser and Natacha Gribenski (University of Stockholm) for use of EMCCD imaging facilities.

References

Aydaş, C., Engin, B., and Aydin, T. *Radiation-induced signals of gypsum crystals analysed by ESR and TL techniques applied to dating*. Nuclear Instruments and Methods in Physics Research, Section B: Beam Interactions with Materials and Atoms, 269(4): 417–424, 2011. doi: 10.1016/j.nimb.2010.12.074.

Detschel, M. and Lepper, K. *Optically stimulated luminescence dating properties of Martian sediment analogue materials exposed to a simulated Martian solar spectral environment*. Journal of Luminescence, 129(4): 393–400, 2009. doi: 10.1016/j.jlumin.2008.11.008.

Duller, G. *Distinguishing quartz and feldspar in single grain luminescence measurements*. Radiation Measurements, 37(2): 161–165, 2003. doi: 10.1016/S1350-4487(02)00170-1.

Fogler, H., Lund, K., and McCune, C. *Acidization III-The kinetics of the dissolution of sodium and potassium feldspar in HF/HCl acid mixtures*. Chemical Engineering Science, 30: 1325–1332, 1975. doi: 10.1016/0009-2509(75)85061-5.

Hilbert, Y., White, T., Parton, A., Clark-Balzan, L., Crassard, R., Groucutt, H., Jennings, R., Breeze, P., Parker, A., Shipton, C., Al-Omari, A., Alsharekh, A., and Petraglia, M. *Epipalaeolithic occupation and palaeoenvironments of the southern Nefud desert, Saudi Arabia, during the Terminal Pleistocene and Early Holocene*. Journal of Archaeological Science, 50(1): 460–474, 2014. doi: 10.1016/j.jas.2014.07.023.

Jain, M., Andersen, C., Bøtter-Jensen, L., Murray, A., Haack, H., and Bridges, J. *Luminescence dating on Mars: OSL characteristics of Martian analogue materials and GCR dosimetry*. Radiation Measurements, 41(7-8): 755–761, 2006. doi: 10.1016/j.radmeas.2006.05.018.

Jungner, H. and Bøtter-Jensen, L. *Study of sensitivity change of OSL signals from quartz and feldspars as a function of preheat temperature*. Radiation Measurements, 23(2-3): 621–624, 1994. doi: 10.1016/1350-4487(94)90110-4.

Kocurek, G., Carr, M., Ewing, R., Havholm, K., Nagar, Y., and Singhvi, A. *White Sands Dune Field, New Mexico: Age, dune dynamics and recent accumulations*. Sedimentary Geology, 197 (3-4): 313–331, 2007. doi: 10.1016/j.sedgeo.2006.10.006.

Lager, G. A., Armbruster, T., Rotella, F. J., Jorgensen, J. D., and Hinks, D. G. *A crystallographic study of the low-temperature dehydration products of gypsum, $CaSO_4 \cdot 2H_2O$: hemihydrate $CaSO_4 \cdot 0.5H_2O$, and $\gamma - CaSO_4$*. The American Mineralogist, 69: 910–918, 1984.

Mahan, S. and Kay, J. *Building on previous OSL dating techniques for gypsum: A case study from Salt Basin playa, New Mexico and Texas*. Quaternary Geochronology, 10: 345–352, 2012. doi: 10.1016/j.quageo.2012.02.001.

Mathew, G., Gundu Rao, T., Sohoni, P., and Karanth, R. *ESR dating of interfault gypsum from Katrol hill range, Kachchh, Gujarat: Implications for neotectonism*. Current Science, 87(9): 1269–1274, 2004.

McLeod, L., Rudowski, R., and Ullman, W. *Pure gypsum separates from 'dirty' evaporites*. Research Methods Papers, pp. 596–597, 1985.

Mees, F., Casteñeda, C., Herrero, J., and Van Ranst, E. *The nature and significance of variations in gypsum crystal morphology in dry lake basins*. Journal of Sedimentary Research, 82(1): 37–52, 2012. doi: 10.2110/jsr.2012.3.

Murray, A. and Wintle, A. *Luminescence dating of quartz using an improved single-aliquot regenerative-dose protocol*. Radiation Measurements, 32(1): 57–73, 2000. doi: 10.1016/S1350-4487(99)00253-X.

Murray, A. and Wintle, A. *The single aliquot regenerative dose protocol: Potential for improvements in reliability*. Radiation Measurements, 37(4-5): 377–381, 2003. doi: 10.1016/S1350-4487(03)00053-2.

Nagar, Y., Sastry, M., Bhushan, B., Kumar, A., Mishra, K., Shastri, A., Deo, M., Kocurek, G., Magee, J., Wadhawan, S., Juyal, N., Pandian, M., Shukla, A., and Singhvi, A. *Chronometry and formation pathways of gypsum using Electron Spin Resonance and Fourier Transform Infrared Spectroscopy*. Quaternary Geochronology, 5(6): 691–704, 2010. doi: 10.1016/j.quageo.2010.05.001.

Nambi, K. *ESR and TL dating studies on some marine gypsum crystals*. PACT, 6: 314–321, 1982.

O'Connor, V., Lepper, K., Morken, T., Thorstad, D., Podoll, A., and Giles, M. *A survey of the signal stability and radiation dose response of sulfates in the context of adapting optical dating for Mars*. Journal of Luminescence, 131(12): 2762–2768, 2011. doi: 10.1016/j.jlumin.2011.06.031.

Petraglia, M., Alsharekh, A., Crassard, R., Drake, N., Groucutt, H., Parker, A., and Roberts, R. *Middle Paleolithic occupation on a Marine Isotope Stage 5 lakeshore in the Nefud Desert, Saudi Arabia*. Quaternary Science Reviews, 30: 1555–1559, 2011.

Petraglia, M., Alsharekh, A., Breeze, P., Clarkson, C., Crassard, R., Drake, N., Groucutt, H., Jennings, R., Parker, A., Parton, A., Roberts, R., Shipton, C., Matheson, C., Al-Omari, A., and Veall, M.-A. *Hominin dispersal into the Nefud Desert and Middle Palaeolithic Settlement along the Jubbah Palaeolake, Northern Arabia*. PLoS ONE, 7(11): e49840, 2012.

Richter, D., Richter, A., and Dornich, K. *Lexsyg A new system for luminescence research*. Geochronometria, 40(4): 220–228, 2013. doi: 10.2478/s13386-013-0110-0.

Spooner, N. *On the optical dating signal from quartz*. Radiation Measurements, 23(2-3): 593–600, 1994. doi: 10.1016/1350-4487(94)90105-8.

Thiel, C., Buylaert, J., Murray, A., Terhorst, B., Hofer, I., Tsukamoto, S., and Frechen, M. *Luminescence dating of the Stratzing loess profile (Austria) - Testing the potential of an elevated temperature post-IR IRSL protocol*. Quaternary International, 234(1-2): 23–31, 2011. doi: 10.1016/j.quaint.2010.05.018.

Warren, J. *Evaporites: Sediments, resources, and hydrocarbons*. Springer, Berlin, 2006. ISBN 9783540260110.

Reviewer

Shannon Mahan